Optical bistability in the mixed absorptive-dispersive regime with two-state atoms

L. A. Orozco, A. T. Rosenberger,* and H. J. Kimble
Department of Physics, University of Texas, Austin, Texas 78712
(Received 3 June 1987)

Quantitative comparisons between experiment and theory for the steady-state characteristics in optical bistability with two-state atoms are reported. Nonresonant conditions for both the cavity and the atomic medium are investigated in two different cavity geometries (ring and standing wave). The experiment fulfills to a very good degree the conditions that have been widely employed in theoretical models that consider a collection of two-state atoms interacting with a single mode of the electromagnetic field in a cavity.

INTRODUCTION

The development of the theory of optical bistability with two-state atoms over the last decade[1] focused very early on the two distinct regimes of absorptive and dispersive bistability. In the former case the atoms are driven on resonance while in the latter they are driven very far from resonance neglecting any absorption. Both limits present hysteresis as a function of incident driving intensity, but the physical origins of the hysteresis are quite different. Atomic saturation in the absorptive case can switch the cavity transmission from a low to a high state, while the intensity-dependent index of refraction shifts the cavity resonances for the dispersive case. These models were fundamental in understanding the pioneering experiments in the field.[2]

As time passed and more questions were asked, it became clear that the transverse profile of the field and the broadening mechanisms of the atomic medium play an important part in modifying the threshold powers for the onset and development of hysteresis.[3(a),3(b)] Then the study of the dynamics[4] of the system with comparable decay rates for the atomic polarization and the cavity mode, keeping the absorptive and dispersive contributions, showed rich dynamical behavior.[1,5] Recent analysis of the quantum statistics of the transmitted light in the regime explored in this paper have shown oscillatory exchange of excitation[6] and significant degrees of squeezing in the lower branch of optical bistability.[7(d)]

We have performed experiments in absorptive optical bistability[7(a)–7(c),8] in a system that to a very good approximation is a collection of radiatively broadened two-state atoms interacting with a single mode of a cavity. The system is well characterized and allows us to make absolute comparisons with theory. We have extended our study to the nonresonant case when either the cavity alone or both the atoms and the cavity are driven off resonance in a regime where absorptive and dispersive contributions are present. Results for those cases are reported here and absolute comparisons with theory made.

EXPERIMENTAL APPARATUS

Our experimental apparatus (Fig. 1) consists of a set of ten well-collimated optically prepumped atomic beams of sodium which intersect the axis of a high-finesse interferometer at 90°.[7] The atoms are prepared[9] in the $3\,^2S_{1/2}$, $F=2, m_F=2$ state and are excited with circularly polarized light to the $3\,^2P_{3/2}, F=3, m_F=3$ state of the D_2 line. The measured absorption width of 13 MHz is greater than the 10 MHz natural linewidth primarily because of transit broadening. Experiments are performed using the following two distinct interferometer geometries: confocal ring[7(b),8] and out-of-confocal standing wave.[7(c)] Both geometries are derived from a basic resonator formed by two 1.27-cm-diam mirrors with a 5-cm radius of curvature. The separation of the mirrors is 5.0 cm for the confocal ring, giving a free spectral range (FSR) of 1.5 GHz, and 5.5 cm for the standing-wave cavity with 2.7 GHz FSR. Both cavities have a mode waist w_0 of approximately 69 μm. Two different sets of mirrors are used, one for the ring cavity only and the other for both ring and standing-wave cavities. Experiments reported here are all done using the second set of mirrors with transmission coefficients $T_1=T_2=(3.0\pm0.1)\times10^{-3}$. To measure the cavity loss and enhancement we need the finesse F [FSR divided by the fullwidth at half maximum (FWHM)] and the resonant cavity transmission T_0.[10] Their values are $T_0=(6.6\pm0.3)\times10^{-2}$, $F=263\pm15$ for the confocal ring and $T_0=0.30\pm0.02$, $F=650\pm30$ for the standing-wave cavity. The incident laser is mode-matched to the fundamental TEM_{00} mode of the cavities with an efficiency greater than 94%. The ring configuration is mode degenerate while the standing-wave cavity has its first higher-order transverse mode offset more than 30 cavity linewidths from the fundamental TEM_{00} mode.

The excitation source for the cavity is a commercial frequency and intensity stabilized cw dye laser with an approximate rms linewidth of 500 kHz. The power entering the cavity (P_i) is measured by splitting a constant fraction onto a photodiode calibrated to the power

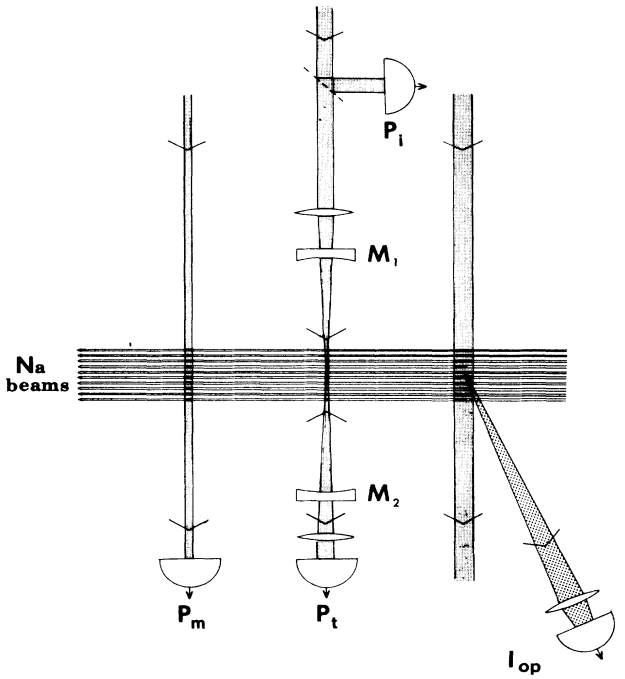

FIG. 1 Experimental setup. Three laser beams (fine shade) intersect ten well-collimated atomic beams of sodium at 90°. The first laser optically prepumps the atoms into the $3S_{1/2}, F=2, m_F=2$ state of the D_2 line, with the fluorescence (grainy shade) from one of the center beams (I_{op}) collected onto a photomultiplier tube. The second laser (signal beam) is mode matched to the cavity formed by mirrors $M1$ and $M2$. The input power (P_i) is measured by splitting a constant fraction onto a photodiode while the output power (P_t) transmitted through the cavity is detected by a photomultiplier tube. Further downstream the small-signal absorption is measured with the monitor beam (P_m). The transverse dimensions of the laser beams relative to the atomic beams are exaggerated in the figure.

incident upon the cavity with an absolute accuracy of ±5%. The output power transmitted (P_t) through the cavity is detected by a photomultiplier tube which is also calibrated. Measurements of the small-signal absorption $\alpha_m l$ are performed before each experiment and related to the optical pumping fluorescence (I_{op}) and to another small absorption signal measured downstream from the cavity (P_m) (Fig. 1), in order to calibrate the intracavity absorption during the experiment in terms of I_{op} and P_m.

For the experiments the atomic density is varied gradually while the input intensity is modulated at 50 Hz. This rate is many orders of magnitude slower than any of the dynamic rates of the system, thereby ensuring the observation of steady-state behavior. The input-output characteristics (P_t versus P_i) are continuously recorded. For the off-resonant experiments, the laser is tuned away from the atomic line center and the optical pumping fluorescence, the line profile of which has been previously calibrated, is measured to determine the atomic detuning. An independent interferometer is continuously scanned to provide further information on the laser detuning with respect to the atomic line center. Care is taken not to detune very far from the atomic resonance, since that could reduce the efficiency of the optical pumping. An intensity of 45 mW/cm^2 over a distance of 3 mm is used for optical pumping and the atomic detuning is kept within ±15 MHz of line center. Cavity detuning is achieved by varying the voltage applied to a piezoelectric crystal PZT which controls the position of the input mirror of the cavity $M1$. The measurement of the detuning is made by comparing the slope of the input-output response high on the upper branch of the bistable curve, where the atoms are saturated, with the resonant empty cavity slope. It is a direct measurement of the detuning, provided one is on a sufficiently high section of the upper branch; it does not depend on detector calibrations. As a cross check for the cavity detuning we monitor the voltage applied to the PZT when it is on resonance and off resonance and compare these values to the transmission-voltage characteristic of the empty cavity. This technique provides knowledge of the sign of the detuning. Good agreement is obtained between the values inferred from the two methods.

MODEL

Agrawal and Carmichael,[11] among others,[1] carried out an extensive study for nonresonant optical bistability. Their model considered a medium of homogeneously broadened two-level atoms in a Fabry-Perot interferometer with plane waves and in the mean-field approximation. They explored the parameter dependence of the hysteresis cycle and mapped it to create a global picture of the five-dimensional parameter space. Drummond[12] included the Gaussian transverse profile in ring and standing-wave cavities based on a fully quantized Hamiltonian using a semiclassical decorrelation. His state equation relates Y (the normalized intracavity intensity in the absence of the atomic medium) to X (the normalized intracavity intensity in the presence of atoms) as a function of the cooperativity parameter C (one-half the ratio of atomic loss to cavity loss), atomic detuning Δ (measured in units of the polarization decay rate $\gamma_\perp$), and cavity detuning Θ (measured in units of the cavity decay rate κ). The state equation is derived assuming Lorentzian homogeneous broadening and arbitrary inhomogeneous broadening. For comparison with our experimental results it is necessary to take into account the main broadening mechanism in our system, which is the transit of atoms through the Gaussian beam, that falls into neither category. An atom with the most probable speed crosses the beam $2w_0$ in approximately 12 radiative lifetimes. For the work in absorptive bistability[7(c)] a detailed calculation involving the numerical integration of the Maxwell-Bloch equations was carried out. We have shown[8] that the difference between the full calculation and a simple approximation of transit broadening as a homogeneous process is less than 10% for the input switching point in the lower branch and 3% for the input switching point in the upper branch of absorptive bi-

stability in our experiment. Calculations taking nonzero Δ and Θ into account show approximately the same degree of agreement with the homogeneous treatment as the resonant absorptive case. Thus comparisons with theory are made using Drummond's state equation modifying $\gamma_\perp/2\pi$ from 5 MHz (purely radiative) to 6.2 MHz (homogeneous treatment of transit broadening) and the saturation intensity (I_s) from 6.4 to 7.3 mW/cm^2. We neglect the remnant Doppler broadening due to finite collimation.

With this motivation we take the state equation for the ring cavity to be [Ref. 12, Eq. (9)]

$$Y=X\left[1+\frac{C}{X}\ln\left[1+\frac{2X}{1+\Delta^2}\right]\right]^2 +X\left[\Theta-\frac{C\Delta}{X}\ln\left[1+\frac{2X}{1+\Delta^2}\right]\right]^2 \tag{1a}$$

and for the standing-wave cavity [Ref. 12, Eq. (10)]

$$Y=X\left\{1+\frac{3C}{X}\ln\left[\frac{1}{2}+\frac{1}{2}\left[1+\frac{8X}{3(1+\Delta^2)}\right]^{1/2}\right]\right\}^2 +X\left\{\Theta-\frac{3C\Delta}{X}\ln\left[\frac{1}{2}+\frac{1}{2}\left[1+\frac{8X}{3(1+\Delta^2)}\right]^{1/2}\right]\right\}^2 \tag{1b}$$

with

$$Y=f_1\frac{T_0P_i}{\pi w_0^2 I_s T_2},\quad X=f_1\frac{P_t}{\pi w_0^2 I_s T_2},\quad C=f_2\frac{\alpha_m lF}{2\pi}, \tag{2}$$
$$\Theta=\frac{\omega_c-\omega_l}{\kappa},\quad \Delta=\frac{\omega_a-\omega_l}{\gamma_\perp},$$

where $f_1=1$ and $f_2=\frac{1}{2}$ for the ring cavity, while $f_1=3$ and $f_2=1$ for the standing-wave cavity; ω_l is the frequency of the driving field, ω_a is the resonant frequency of the atoms, and ω_c is the nearest resonant frequency of the cavity with respect to the driving field.

RESULTS

Figure 2 presents the ratio $R=Y_2/Y_1$ of input switching points (Y_2 where the system jumps from the lower to the upper branch and Y_1 where it switches back down to the lower branch) for the ring cavity as a function of cavity detuning in the case of atomic resonance ($\Delta=0$). Note that R is independent of systematic errors in the calibration of input intensity. For this set of data, systematic problems in the experiment prevent us from making an absolute comparison with theory of the scaled input switching intensities (Y_1, Y_2); however, the input ratio scales well with the cooperativity C in the absorptive case. The value of C directly determined using Eq. (2) with measured quantities is 15 ± 1.5 and agrees well (within our $\pm10\%$ systematic uncertainty) with the value of C determined from the ratio R in resonant absorptive bistability, which is used to generate the solid curve from Eq. (1a).

Figure 3 presents a detailed comparison of the normalized input switching intensities as a function of cavity detuning Θ for the standing-wave cavity. All values are measured quantities with a systematic uncertainty of $\pm20\%$ in Y and $\pm10\%$ in C. The value of C to generate the solid curve from Eq. (1b) was determined as in Fig. 2. For comparison using Eq. (2) and measured quantities, we find $C=16\pm1.6$. The theoretical predictions from Eq. (1b) of Y are scaled by 0.91 to obtain the best agreement at the resonant point $\Theta=0$.

The role of atomic detuning is explored in Figs. 4 and 5. Both figures present absolute comparisons of the in-

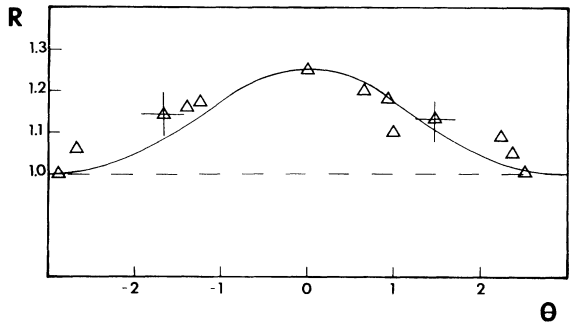

FIG. 2. Ratio R of input switching intensities Y_2/Y_1 as a function of cavity detuning Θ for $\Delta=0$ and $C=16$ in the ring cavity. The solid line is the theoretical prediction from Eq. (1a) without adjustment.

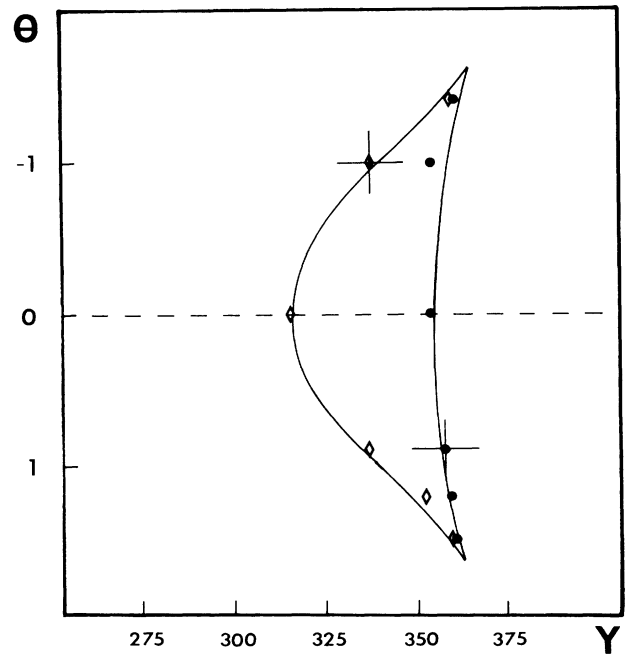

FIG. 3. Normalized input switching intensities Y_1 (rhombs) and Y_2 (dots) for the standing-wave cavity as a function of cavity detuning Θ with no atomic detuning $\Delta=0$ and $C=15$. The solid line is the theoretical prediction for Y scaled down by a factor of 0.91, which is within our experimental uncertainties.

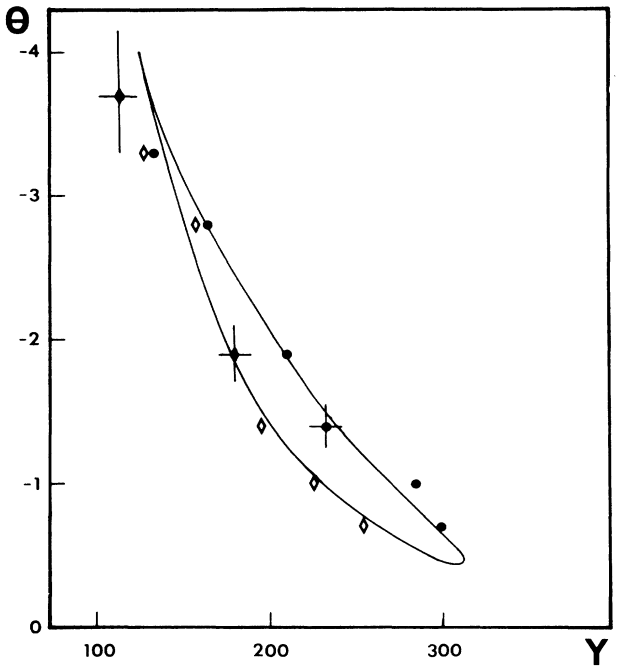

FIG. 4. Normalized input switching intensities Y_1 (rhombs) and Y_2 (dots) ($\pm 20\%$) for the standing-wave cavity as a function of cavity detuning Θ with atomic detuning $\Delta = -2 \pm 0.2$ and $C = 15$. The lines represent the theoretical prediction with Y scaled down by 0.91, a factor within our experimental uncertainty.

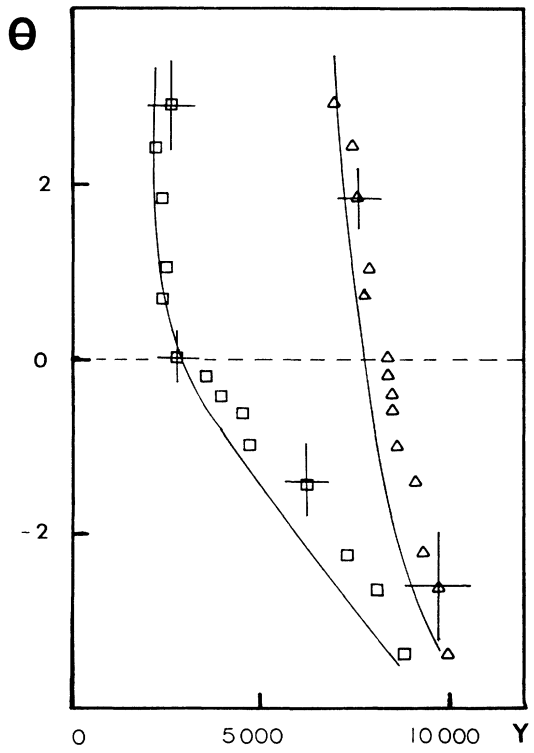

FIG. 5. Normalized input switching intensities Y_1 (squares) and Y_2 (triangles) ($\pm 10\%$) for atomic detuning with $\Delta = 1.0 \pm 0.2$ and $C = 72 \pm 7$ as a function of cavity detuning Θ for the standing-wave cavity. The solid lines are theoretical predictions without adjustment.

put switching points ($\pm 20\%$ in Fig. 4 and $\pm 10\%$ in Fig. 5) as a function of cavity detuning ($\pm 10\%$) for fixed atomic detuning. The data are from experiments with the standing-wave cavity. In Fig. 4 the value of $C = 15$ for the solid curve was determined by matching C to the ratio of input switching points in the absorptive case while we find $C = 16 \pm 1.6$ from measured quantities and Eq. (2). The normalized switching points Y obtained from Eq. (1b) are scaled by 0.91. This factor brings the experiment into agreement with the theory in the absorptive case and is within our experimental uncertainty. Figure 5 has no scaling in Y and the value of C is that determined directly from measured quantities and Eq. (2). Equation (1b) was used to calculate the solid curve.

Finally, Fig. 6 presents another "phase diagram" for the limits of hysteresis in the (Θ, C) plane for fixed atomic detuning in the ring cavity. Our systematic uncertainties in C and Θ are $\pm 10\%$. The theoretical curve is directly determined from Eq. (1a) without any scaling.

CONCLUSIONS

We have explored in quantitative detail the parameter space of optical bistability with two-state atoms when both the cavity and atoms are driven off resonance and both absorptive and dispersive nonlinearities are present. The observations are in two different cavity geometries. The first is a ring configuration which is intrinsically mode degenerate and the second is an out-of-confocal

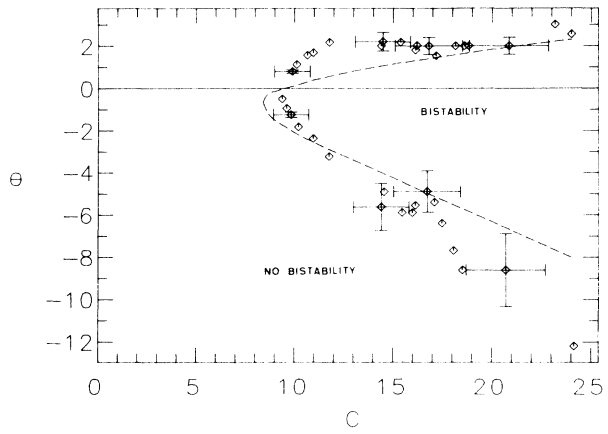

FIG. 6. Phase diagram for hysteresis in the (C, Θ) plane for atomic detuning $\Delta = -0.75 \pm 0.25$ in the ring cavity. Both scales have overall uncertainties of $\pm 10\%$. The data points limit the existence of bistability as one detunes the cavity away from resonance. The curve represents the theoretical prediction without adjustment.

standing-wave cavity which should be a single-mode cavity both with respect to longitudinal and transverse modes. The agreement in absolute terms with a theory of homogeneously broadened two-level atoms in a single-mode cavity is good within our experimental uncertainties. The results show that the mode degeneracy of the confocal resonator does not affect the good quantitative agreement with theory when the atomic and cavity detunings are kept small. For higher detunings we have observed transverse mode switching on the upper branch of the hysteresis curve when the product $\Delta\Theta$ is positive in the confocal resonator.

The curves we have presented represent "phase diagrams" obtained by different cuts in the parameter space of the surface defined by the state equation. This experiment provides a foundation for future absolute comparisons between experiment and theory in studies of quantum phenomena in off-resonant optical bistability. Furthermore, it represents one of a very few experiments to have made absolute contact with theory in studies of the critical behavior of nonequilibrium optical systems.

ACKNOWLEDGMENTS

We would like to thank Professor H. J. Carmichael for many valuable discussions. L. A. Orozco acknowledges support from IBM. Funding was provided by the U.S. National Science Foundation, the Venture Research Unit of British Petroleum North America, Inc., and the Joint Services Electronics Program.

---

*Present address: Department of Physics, Southern Methodist University, Dallas, TX 75275.

[1]L. A. Lugiato, in *Progress in Optics,* edited by E. Wolf (North-Holland, Amsterdam, 1984), Vol. 21, p. 69.

[2]H. M. Gibbs, S. L. McCall, and T. N. C. Venkatesan, Phys. Rev. Lett. **36**, 1135 (1976).

[3](a) W. J. Sandle and A. Gallagher, Phys. Rev. A **24**, 2017 (1981); (b) S. L. McCall, *ibid.* **9**, 1515 (1974).

[4]J. C. Englund, R. R. Snapp, and W. C. Schieve, in *Progress in Optics,* edited by E. Wolf (North-Holland, Amsterdam, 1984), Vol. 21, p. 355.

[5]L. A. Lugiato, R. J. Horowicz, G. Strini, and L. M. Narducci, Phys. Rev. A **30**, 1366 (1984).

[6]H. J. Carmichael, Phys. Rev. A **33**, 3262 (1986).

[7](a) D. E. Grant and H. J. Kimble, Opt. Lett. **7**, 353 (1982); (b) A. T. Rosenberger, L. A. Orozco, and H. J. Kimble, Phys. Rev. A **28**, 2569 (1983); (c) L. A. Orozco, H. J. Kimble, and A. T. Rosenberger, Opt. Commun. **62**, 54 (1987); (d) M. G. Raizen, L. A. Orozco, Min Xiao, T. L. Boyd, and H. J. Kimble, Phys. Rev. Lett. **59**, 198 (1987).

[8]A. T. Rosenberger, L. A. Orozco, H. J. Kimble, and P. D. Drummond (unpublished).

[9]J. A. Abate, Opt. Commun. **10**, 269 (1974); M. L. Citron, H. R. Gray, C. W. Gabel, and C. R. Stroud, Jr., Phys. Rev. A **16**, 1507 (1977).

[10]A. T. Rosenberger, L. A. Orozco, R. J. Brecha, and H. J. Kimble (unpublished).

[11]G. P. Agrawal and H. J. Carmichael, Phys. Rev. A **19**, 2074 (1979).

[12]P. D. Drummond, IEEE J. Quantum Electron. **QE-17**, 301 (1981).